Journal of Metals, Materials and Minerals. Vol.16 No.2 pp.19-23, 2006

Techniques to Improve Coating Adhesion of Superhard Coatings

Nurot PANICH[1], Panyawat WANGYAO[1*], Nuntapol VATTANAPRATEEP[2] and Sun YONG[3]

[1] Metallurgy and Materials Science Research Institute, Chulalongkorn University, Bangkok, Thailand
[2]Dept. of Industrial Engineering, Faculty of Engineering, Rajapark College, Thailand
[3] School of Engineering & Technology, De Montfort University, Leicester LE1 9BH, UK

Received Oct. 5, 2006
Accepted Nov. 1, 2006

Abstract

This work addresses the development of different techniques in fabricating TiB_2 coatings with increased adhesion to the substrate and with retained high hardness. Titanium diboride (TiB_2) coatings were deposited on high-speed steel substrates by magnetron sputtering of a TiB_2 target. Attempts to enhance the coating adhesion to the substrate of the TiB_2 coatings by controlling the deposition conditions and parameters are presented, such as effect of substrate rotation; annealing temperature; using deposited Cr as an interlayer material and Ti/TiB_2 multilayer system. The structure of the coatings was examined by X-ray diffraction, field-emission scanning electron microscopy, and atomic force microscopy. The coating hardness and coating-substrate adhesion were investigated by nanoindentation and micro-scratch tests. It was found that the adhesion of resultant TiB_2 coatings was increased tremendously by stationary substrate during deposition; annealing at optimal temperature of 450°C; using Cr interlayer and increased alternate TiB_2/Ti layers.

Key words: titanium diboride coating, magnetron sputtering, adhesion and micro-scratch

Introduction

Titanium diboride (TiB_2) is well known as a ceramic compound with a hexagonal crystal structure and with relatively high strength and durability as characterised by its relatively high melting point, hardness, strength to density ratio, abrasion, oxidation resistance and wear resistance.[1, 2] Recently, one of the major uses of TiB_2 is as a wear resistant material in such areas as impact resistant armor, cutting tools, bearings, sandblasting nozzles, crucibles, and wear resistant coatings.[1, 3] Although TiB_2 coatings have been widely studied by many researchers, their real applications have been very limited. The fact is that the adhesion of the TiB_2 coatings is poor for the coating-substrate system. The main reasons for this are that the TiB_2 coating deposited is very brittle and that it accommodates very high compressive residual stresses. These limit both the practical adhesion and the thickness of the TiB_2 coatings.[4] Actually, the adhesion of the coating is the most critical aspect of the coating-substrate system and adhesion theories generally do not provide guidelines on how to achieve good film or coating adhesion in practice. Conventional wisdom, for example, suggests using very clean substrates. However, this may not necessarily work for metal films on glass substrates because optimum adhesion appears to occur only when the metal contacts the substrate through an oxide bond.[5]

In the present investigation, attempts have been made to fabricate TiB_2-based nanostructured engineering coatings on high speed steel substrate with the techniques to enhance its coating adhesion. The characterization of their structures and properties has been studied.

Experimental Procedure

High speed steel (HSS) was chosen as a substrate in this study. The commercial HSS, SECO WKE45 (Sweden) was in a fully hardened and tempered condition. The tempering temperature of the HSS was about 600ºC. The chemical composition (wt.%) of the HSS substrate is shown in Table 1.

e-mail: panyawat@hotmail.com

High-purity argon gas was then introduced into the chamber after it was evacuated to below 5×10^{-4} Pa. All targets i.e. TiB_2, Ti and Cr, were 75 mm diameter and 5 mm thickness. The two TiB_2 targets were powered in the radio frequency (rf) mode and the metallic Ti and Cr target were powered in the direct current (dc) mode. Then the targets were pre-sputtered with the target shutters closed. The working table was rotating (6 rpm) and stationary during the deposition process. The substrate to target distance was held constant at 100 mm for dc target (Ti and Cr) and at 60 mm for rf target (TiB_2). All the experiments were conducted at a constant working pressure of 0.65 Pa and at a total gas flow rate (Ar) of 20 sccm. The substrate temperature was 400ºC for all depositions. A RF power biased to the substrate was used to sputter clean the substrate surface and provide substrate bias at different levels for some depositions. A thin (about 50 nm) pure Ti interlayer was deposited first in the cases of using Ti as an interlayer. Table 2. summarises the deposition conditions and parameters presented, such as effect

Table 1. Chemical composition of high-speed steel (wt.%)

Element	C	Cr	W	Mo	V	Co	Fe
Content (wt.%)	1.4	4.2	9	3.5	3.5	12.5	Balance

Table 2. Deposition conditions and properties of resultant coatings

Materials	**Substrate rotation**	**Deposition details**	**Sputter-cleaning of substrate**	**Coating thickness (micron)**	**H* (GPa)**	**E** (GPa)**	**L_c *** (mN)**
Effect of substrate rotation							
Sample 1	rotating	Ti 20 min + TiB_2 300 min	No	2.5	20.4	297.9	880
Sample 2	stationary	Ti 20 min + TiB_2 200 min	No	2.5	42.7	368.2	2,153
Effect of heat treatment							
Sample 3	stationary	Ti 30 min + TiB_2 180 min	150 W 30 min	1.98	31.6	321.3	1,089
Sample 4	stationary	Ti 30 min + TiB_2 180 min & annealed at 450 ºC (2 h)	150 W 30 min	1.83	41.9	338.3	2,596
Sample 5	stationary	Ti 30 min + TiB_2 180 min & annealed at 500 ºC (2 h)	150 W 30 min	1.67	38.8	326.6	1,880
Sample 6	stationary	Ti 30 min + TiB_2 180 min & annealed at 550 ºC (2 h)	150 W 30 min	1.67	38.7	305.8	1,653
Effect of Cr interlayer							
Sample 7	stationary	Ti 20 min + TiB_2 180 min	150 W 90 min	1.75	34.3	329.5	1,240
Sample 8	stationary	Cr 20 min + TiB_2 180 min	150 W 90 min	1.7	36.3	303.1	2,034
Effect of multilayer							
Sample 9	stationary	2 (Ti 20 min + TiB_2 90 min)	150 W 90 min	2.52	33.4	340.2	1,855
Sample 10	stationary	3 (Ti 20 min + TiB_2 60 min)	150 W 90 min	3.15	35.6	365.4	1,995
Sample 11	stationary	6 (Ti 20 min + TiB_2 30 min)	150 W 90 min	3.42	20.1	126.4	1,650

* H = hardness, ** E = Reduced modulus, *** L_c = Critical load to coating failure

of substrate rotation; annealing temperature; using deposited Cr as an interlayer material and Ti/TiB_2 multilayer system.

The phase identification of the resultant coatings was determined by Rigagu x-ray diffractometer with Cu-Kα radiation. Crystallographic phases were deduced by comparing the experimental diffraction pattern with the standard JCPDS data. The morphologies of surfaces and fractured cross-sections of the coatings were imaged using a field emission scanning electron microscope (FESEM), Jeol JSM 6340F. A tungsten tip was heated and a 5 kV accelerating voltage was applied to release electrons in the SEM measurements. The emission current was 12 mA during operating and the working distance was about 8 mm.

A nanoindentation test was performed using the NanoTest™ instrument (Micro Materials Limited, UK), with a Berkovich diamond indenter. All experiments were performed at a constant loading and unloading rate of 0.05 mN/s and to a penetration depth of 50 nm. The unloading curves were used to derive the hardness and reduced modulus values by the analytical technique developed by Oliver and Pharr.[6] The reported hardness and modulus values are the average of 10 measurements. The micro-scratch test was performed using a NanoTest™ device as well with an indenter topped with a conical with spherical end form of 25 μm in radius. The stylus was moved tangential to the surface at a speed of 5 μm/s over a length of 3,050 μm. At the same time, the applied load was increased linearly at a rate of 5 mN/s from 0 to 500 mN. All scratch tests were performed at ambient temperature.

Results and Discussion

Structural characterization Figure. 1 shows the X-ray diffraction patterns recorded for the selected coatings listed in Table 2. Each pattern shows several broad reflection peaks corresponding to the hexagonal TiB_2 structure. The broadness of the reflected peaks indicates the nanocrystalline nature of the coating structure.

From Figure.1, it is noted that the TiB2 coatings deposited on rotating substrates (sample 1) did not show any preferred orientation, whilst the coatings on stationary substrates (sample 2) showed strong (001) orientation, with the basal plane parallel to the substrate surface. The increase of preferred (001) orientation can be explained by an increased energy of the sputtered species arriving at the substrate surface. Furthermore, from the XRD test of all samples, it can be concluded that the increase of preferred (001) orientation can be obtained by annealing, whilst the use of Cr as an interlayer material does not significantly affect the preferred (001) orientation TiB_2 coating. On the other hand, the preferred (001) peak decreases with the increase of the alternate layers (decrease of TiB_2 layers) in particular, sample 11 (12 layers).

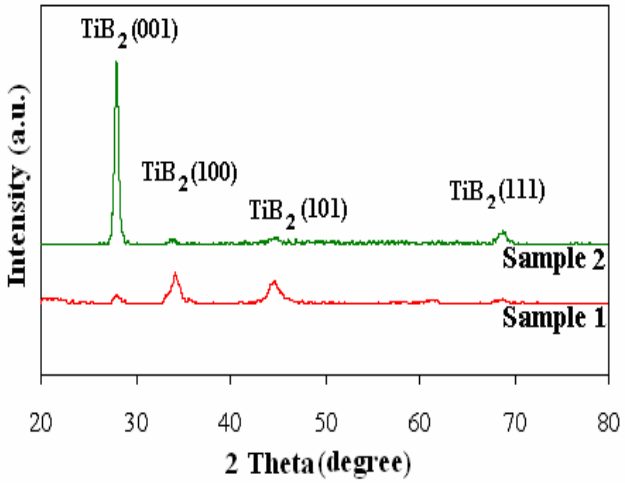

Figure 1. XRD patterns recorded for the coatings studied

The fractured cross-sections of all samples were examined under FESEM, as shown for the selected samples in Figure 2. It is obvious that the thin Ti interlayer could be observed in all samples. From Figure 2, it is seen that the single TiB_2 coating with an interlayer under substrate stationary exhibits a dense and nearly equixed grain structure (Figure. 2(a)), whilst the multilayer coatings (samples 9-11) show a columnar structure (Figure.2(b)), which is typical of sputter deposition at relatively low adatom energies and limited mobility. This observation indicates that sufficient time is required for the TiB_2 layer to develop into a dense and equiaxed structure, and interrupting the growth of the TiB_2 layer with a Ti interlayer obstructs the development of such a structure and favours the columnar growth of TiB_2.

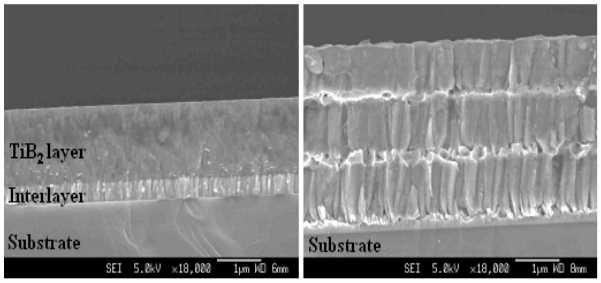

(a) Dense structure (sample 8) (b) Columnar structure of multilayer (6 layers, sample 10)

Figure 2. FESEM images showing the fractured cross-section of (a) sample 8 and (b) sample10

Mechanical properties

Coating hardness. The hardness and reduced modulus values measured by nanoindentation of all samples are summarised in Table 2. It is seen that all samples under stationary substrate show high hardness (above 30 GP_a) and reduced modulus (above 300 GP_a) except the sample 11 (12 alternate layers). The reduced hardness of sample 11 is due to the effect of soft Ti interlayer, which the measured thickness of TiB_2 on the top layer and in each layer was around 300 nm for sample 11. This indicates that the thickness of TiB_2 coatings mainly results in the hardness value. In addition, the coating under the substrate rotation (sample 1) shows a low hardness, which could be explained by the small peak of preferred (001) texture in Figure 1.

Coating adhesion. The critical load to the coating failure values measured by micro-scratch test of all samples are summarised in Table 2. Figure. 3 (a) shows the typical scratch friction force curves recorded for sample 1 (rotating substrate) and sample 2 (stationary substrate). Each friction curve is characterized by an initial smooth region which increases with increasing load, followed by a region with large fluctuation. The critical load at the transition between these two regions coincides with that measured by the surface profile, and thus corresponds to the critical load for coating adhesive failure (L_C). Clearly, the coating on stationary substrate (sample 2) possesses much higher critical loads than those on rotating substrate (sample 1).

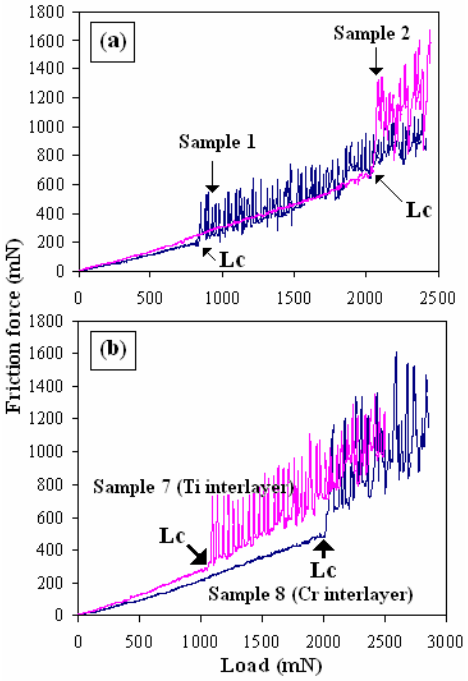

Figure 3. Friction force curves recorded during micro-scratch test for sample 1 and sample 2 (a) and sample 7 and sample 8 (b).

From Table 2, it is seen that coating adhesion is enhanced significantly by heat treatment after deposition. It was found that annealing at an optimum temperature of 450°C (sample 4) shows the most improvement of adhesion by having the highest critical load value compared to annealing at 500°C and 550°C. From Figure. 3 (b), it is seen that a Cr interlayer (sample 8) is more beneficial in further enhancing the adhesion of TiB2 coating compared to a Ti interlayer (sample 7) on HSS substrate. Such an enhancement could be explained by the increased interlayer strength and the better structural match between the BCC interlayer and the BCC-HSS substrate. From Table 2, clearly the multilayer Ti/TiB_2 coatings (samples 9, 10 and 11) possess much higher critical load than the conventional two-layer coating (sample 7). Interestingly, the critical load initially increases an with increasing number of layers, reaching a maximum with the six- layer coating (sample 10), and then decreases with a further increase in the number of layers to twelve (sample 11). Thus, there exists an optimum combination of alternate layers that gives the optimal enhancement in coating adhesion.

Summary

Under the present deposition conditions, the main results are summarized below.

1. The TiB_2 coatings deposited on rotating substrates are characterized by random orientation, columnar growth, relatively low hardness and adhesion strength. On the other hand, without substrate rotation, the resultant coatings exhibit the beneficial (001) orientation, dense and equiaxed grain structure, and enhanced hardness and adhesion strength.

2. It was found that heat treatment at an optimum temperature of 450°C shows the most improvement of mechanical properties (hardness, elastic modulus and adhesion).

3. The adhesion can be significantly enhanced by the Cr interlayer due to the increased interlayer strength and the better structural match between the BCC-Cr interlayer and the BCC-HSS substrate.

4. Magnetron sputtering of Ti and TiB2 can be used to produce multilayer coatings with increased coating adhesion and relatively high hardness.

References

1. Chen, J. and Barnard, J. A . 1995. Growht, structure and stress of sputtered TiB_2 thin films. *Mater. Sci. Eng*. **191(1-2)** : 233-238.

2. Matsubara, E., Waseda, Y., Takeda, S. and Taga, Y. 1990. Structural study of TiB_2 film by grazing incidence X-ray diffraction. *Thin Solid Films* **186 (2)** : L33-L37.

3. Wiedemann, R., Oettel, H. and Jerenz, M. 1997. Structure of deposited and annealed TiB_2 layers. *Surf. Coat. Technol*. **97(1-3)** : 313-321.

4. Berger, M., Larsson, M. and Hogmark, S. 2000. Evaluation of magnetron-sputtered TiB_2 layers. *Surf. Coat. Technol.* **124 (2-3)** : 253-261.

5. Ohring, M. 1991. *The Materials Science of Thin films.* San Diego : Academic Press,.

6. Oliver, W. C. and Pharr, G. M. 1992. *J. Mater. Res*. **7** : 1564

.